JOURNAL OF CRITICAL REVIEWS

ISSN- 2394-5125 VOL 06, ISSUE 07, 2019

Smart Energy Management System for Remote DC Microgrids: Integrating NMPC and MPPT Algorithms for Sustainable Power Supply

G. Ismayel[1], T. Muralikrishna[1], B. Mabu Sarif[1]

[1]Assistant Professor, Dept. of EEE, Malla Reddy Engineering College and Management Sciences, Medchal, Hyderabad, India

Abstract

The main objective of the proposed system is to provide uninterrupted power supply to the load systems, which are located at isolated sites in remote and rural areas. The main goal of the proposed system is to set up an energy management system (EMS) on a DC microgrid using the nonlinear model predictive control (NMPC) and maximum power point tracking (MPPT) algorithms. We suggest a coordinated and flexible EMS that uses a photovoltaic array and a wind turbine as generators that can be controlled by changing the switching duty cycles. Batteries are used as a storage system. The proposed EMS needs to be more flexible with the power curtailment feature in order to achieve a constant current, constant voltage (IU) charging regime and make batteries last longer. Based on each system's MPPTs, the suggested plan is made as a nonlinear model predictive control (NMPC) algorithm. The entire designed system is modeled and simulated using MATLAB/Simulink.

Index terms: *Battery Management, Maximum Power Point Tracking (MPPT), Nonlinear Model Predictive Control (NMPC), Power Sharing, and Voltage Regulation.*

1. INTRODUCTION

Microgrids are new key elements of modern power grids that improve the grids capability of hosting renewable energy and distributed storage systems [1] consisting of ac and dc loads [2]. The near future distribution networks will consist of several interconnected microgrids which will locally generate, consume, and store energy [3]. A microgrid may be operated as an extension of the main grid, i.e., grid-connected, or as a standalone network with no connection to the grid. Standalone dc microgrids have some distinct applications in avionic, automotive, or marine industries, as well as remote rural areas. Due to substantial generation and demand fluctuations in standalone green micro-grids, energy management strategies (EMSs) are becoming essential for the power sharing purpose and regulating the microgrids voltage. The classical EMSs track the maximum power points (MPPs) of wind and PV branches independently and rely on batteries, as slack terminals, to absorb any possible excess energy. However, in order to protect batteries from being overcharged by realizing the constant current, constant voltage (IU) charging regime as well as to consider the wind turbine operational constraints, more flexible multivariable and non-linear strategies, equipped with a power curtailment feature are necessary to control microgrids.

The stability of a dc microgrid is measured in terms of the stability of its dc bus voltage level which is one of the main control objectives [4]. The grid voltage source converters (G-VSCs) are the primary slack terminals to regulate the voltage level of grid-connected microgrids. Battery banks, on the other hand, are effective slack terminals for standalone microgrids [5]. The curtailment strategies [6] of the battery bank which cannot absorb the excess generation restrict the batteries charging rate by the maximum absorbing power; however, the maximum charging current must also be limited. Furthermore, they do not curtail the power of each generator in proportion to its rating. In order to prevent over-stressing conditions and circulating currents between generators [7], load demands need to be shared between all slack DGs in proportion to their ratings [8].

ISSN- 2394-5125 VOL 06, ISSUE 07, 2019

However, standalone dc microgrids are usually located in small-scale areas where the power sharing between DGs can be managed by centralized algorithms which are less affected by two issues: 1) batteries in charging mode are nonlinear loads causing distortions to the grid voltage; and 2) the absolute voltage level of a standalone microgrid is shifted as the result of the load demand variation. A number of phenomena affect the batteries operation during the charging mode [9]: 1) applying high charging currents, the batteries voltages quickly reach to the gassing threshold; 2) the internal resistor and hence power losses and thermal effects increase at high SOC levels; and 3) batteries cannot be fully charged with a constant high charging current and also restricts the maximum attainable SOC that leads to unused capacities [10].

However, since batteries act as nonlinear loads during the charging mode, it does not necessarily limit the charging currents. Depending on the proportion of the power generation to the load demand ratio within standalone DC microgrids, three cases are envisaged: 1) power generation and load demand are balanced; 2) load demand exceeds power generation causes dc bus voltage to drop in absence of any load shedding; and 3) power generation is higher than load demand leads batteries to be overcharged and bus voltage to climb. This study focuses on case 3) in which the generated power must be curtailed if it violates the batteries charging rates or if batteries are fully charged. In contrast to the strategies available in which renewable energy systems (RESs) always operate in their MPPT mode, the proposed multivariable strategy uses a wind turbine and a PV array as controllable generators and curtails their generations if it is necessary. The proposed EMS is developed as an online novel NMPC strategy that continuously solves an optimal control problem (OCP) and finds the optimum values of the pitch angle and three switching duty cycles.

2. SYSTEM DESCRIPTION AND MODELLING

A schematic of the dc microgrid with the conventions employed for power is given in Fig.1. The dc bus connects wind energy conversion system (WECS), PV panels, multilevel energy storage comprising battery energy storage system (BESS) and super capacitor, EV smart charging points, EV fast charging station, and grid interface. The WECS is connected to the dc bus via an ac–dc converter. PV panels are connected to the dc bus via a dc–dc converter. The BESS can be realized through flow battery technology connected to the dc bus via a dc–dc converter. The super capacitor has much less energy capacity than the BESS. Rather, it is aimed at compensating for fast fluctuations of power and so provides cache control as detailed in [10].

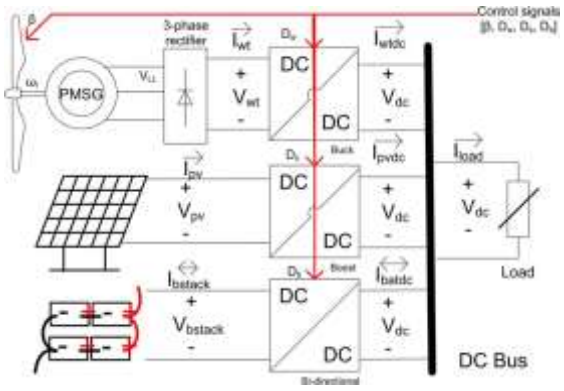

Fig 1. Topology of a small-scale and standalone dc microgrid

The below figure Fig.2 summarizes a modified version of the proposed model. Since this paper focuses on the case in which there is an excess power greater than or equal to the maximum possible absorbing rate of the battery bank the following notations are used to model the standalone dc.

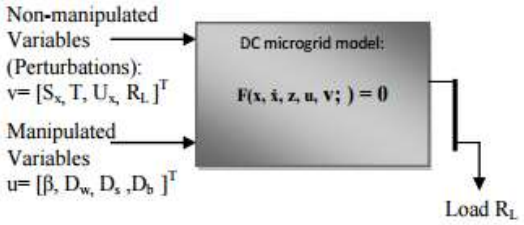

Fig 2 Modified version of the system model

2.1 Modelling of the Three System

Wind Branch: Wind turbines (WTs) convert the kinetic energy of wind to mechanical power. In order to generate the maximum power by a WT at variable wind speed, it is necessary to employ a maximum power point tracking (MPPT) control strategy [11]. A wind turbine can be connected to an electrical generator directly or through a gear-box. In order to convert the three-phase output of a PMSG to dc voltage, it is essential to deploy a three-phase rectifier. A general structure, which consists of a full-bridge diode rectifier connected in series to a dc-dc converter, is common due to lower cost. Performance of the wind turbines is measured as the power coefficient curve with respect to the tip speed ratio and pitch angle. Equation (3) shows the power coefficient curve of three-blade wind turbines.

$$\begin{aligned} f_3 &= C_{p,norm} - \frac{1}{C_{p,\max}} \times \\ &\quad (C_1(\frac{C_2}{\lambda_i} - C_3\beta - C_4)\exp(-\frac{C_5}{\lambda_i}) + C_6\lambda), \\ f_4 &= \lambda - \frac{Rad \times \omega_r}{U_x}, \\ f_5 &= \lambda_i - (\frac{1}{\lambda + 0.08\beta} - \frac{0.035}{\beta^3 + 1})^{-1}, \end{aligned} \tag{3}$$

Where gamma and beta, respectively, are the tip speed ratio and pitch angle. Rad is the radius of the blades and Cp, max is the maximum achievable power coefficient at the optimum tip speed ratio of gamma out. Equation (4) presents the connected PMSG generator

$$\begin{aligned} f_6 &= \frac{d\omega_r}{dt}(t) - \frac{1}{J}(T_e - T_m - F\omega_r), \\ f_7 &= -T_e \times \omega_r - I_{wtdc} \times V_{dc}, \\ f_8 &= -T_m \times \omega_r - (C_{p,norm}(\frac{U_x}{U_{x,base}})^3 P_{nom}. \end{aligned} \tag{4}$$

Energy management strategies of microgrids must estimate the dc bus voltage level deviation from its set point in about every 0.005–0.010 s. It means that except the angular velocity of the generator (4a) all other fast voltage and current dynamics can be ignored. For energy management strategies, the average model of the buck converter is replaced with the steady-state equations for the continuous conduction mode (CCM)

$$\begin{aligned} f_9 &= V_{dc} - D_w V_{wt}, \\ f_{10} &= I_{wt} - D_w I_{wtdc} \end{aligned} \tag{5}$$

Where Dw is the switching duty cycle of the converter and all remaining parameters are as depicted in Fig. 1. The average dc output voltage of the rectifier, Vwt, in presence of the non-instantaneous current commutation is calculated as follows

$$V_{wt} = 1.35V_{LL} - \frac{3}{\pi}\omega_e L_s I_{wt} \tag{6}$$

$$f_{11} = I_{wtdc} - \frac{\pi}{3P\omega_r L_s D_w}\left\{\frac{1.35\sqrt{3}P\psi\omega_r}{\sqrt{2}} - \frac{V_{dc}}{D_w}\right\} \tag{7}$$

Battery Branch: Charging operation of a lead acid battery bank, consisting of (Nbatp*Nbats) batteries, is modelled as:

$$\begin{aligned}
f_{12} &= \frac{V_{bstack}}{N_{bats}} - V_0 + R_{bat}\frac{I_{bstack}}{N_{batp}} + \\
&\quad \frac{P_1 C_{max}}{C_{max} - Q_{act}}Q_{act} + \frac{P_1 C_{max}}{Q_{act} + 0.1C_{max}}I_f, \\
f_{13} &= \frac{dQ_{act}}{dt}(t) - \frac{1}{3600}\frac{I_{bstack}(t)}{N_{batp}}, \\
f_{14} &= \frac{dI_f}{dt}(t) + \frac{1}{T_s}(I_f - \frac{I_{bstack}}{N_{batp}}), \\
f_{15} &= V_{bstack} - \frac{V_{dc}}{1 - D_b}, \\
f_{16} &= I_{bstack} - (1 - D_b)I_{batdc}, \\
f_{17} &= SOC - \left\{1 - \frac{Q_{act}}{C_{max}}\right\}
\end{aligned} \tag{8}$$

The voltage, current and charge state of the battery bank. If the filtered value of the battery current with the time constant of Ts and Qact is the actual battery capacity. The experimental parameter P1 requires being identified for each type of battery while the maximum amount of the battery capacity, Cmax, internal resistor of battery, Rbat, and the battery constant voltage, V0, are given by manufacturers. By ignoring the discharging mode of the battery bank operation, the bi-directional converter acts as a boost type converter.

Solar Branch: PVs are among the popular renewable energy components to harvest solar energy. A PV cell, as the fundamental PV element, is a P-N junction that converts solar irradiance to the electrical energy. Normally, manufacturers provide PV modules, also known as PV panels, which consist of several PV cells connected together in series. A PV cell is a non-linear component that its operation is characterised by a set of current-voltage curves at different insolation levels and junction temperatures. The equivalent electrical circuit of the PV module is used to mathematically model the solar branch, consisting of a PV array and a boost converter [13]. The below equations shows the characteristic equations of a PV array, consisting of Npvp × Npvs PV modules:

$$\begin{aligned}
f_{18} &= I_{pv} - I_{ph} + \\
&\quad I_0\left\{\exp\left(\frac{V_{pv} + \frac{N_{pvs}}{N_{pvp}}R_s I_{pv}}{n_d N_s}\frac{q \times N_{pvs}}{KT_c}\right) - 1\right\} + \\
&\quad \frac{V_{pv} + \frac{N_{pvs}}{N_{pvp}}R_s I_{pv}}{\frac{N_{pvs}}{N_{pvp}}R_{sh}}, \\
f_{19} &= I_{ph} - N_{pvp} \times \\
&\quad \left(\frac{R_s + R_{sh}}{R_{sh}}I_{sc,stc} + k_I\left(T_c - T_{c,stc}\right)\right)\frac{S}{S_{stc}}, \\
f_{20} &= I_0 - N_{pvp} \times \\
&\quad \frac{I_{sc,stc} + k_I\left(T_c - T_{c,stc}\right)}{\exp\left(\frac{V_{oc,stc} + k_V\left(T_c - T_{c,stc}\right)}{n_s N_s}\frac{q}{KT_c}\right) - 1}
\end{aligned} \tag{9}$$

Where Iph denotes the photocurrent and I0 is the diode reverse saturation current. Rs and Rsh, respectively, are the series and parallel equivalent resistors of each PV module.

3. CONTROLLER DESIGN

Maximum Power Point Tracking: Maximum power point tracking (MPPT) is a technique used commonly with wind turbines and photovoltaic (PV) solar systems to maximize power extraction under all conditions. The MPPT technique is also useful for the operation of battery. Depending upon the MPPT technique charging and discharging modes of operations of batteries are controlled. It is useful in protecting the battery from over charging, and to implement the IU charging regime of the battery that helps to increase the life span of batteries. The output power induced by the pv modules and wind turbine are influenced by number of factors which are solar radiation, temperature, wind speed etc. To maximize the power output from the system it is necessary to track the maximum power points of the individual energy sources. There are several methods to track the mpp's of the system among them P&O is the commonly used method.

Nonlinear Model Predictive Control (NMPC): Non-linear model predictive control (NMPC) strategies are inherently multivariable and handle constraints and delays. In this thesis, the EMS is developed as a NMPC strategy to extract the optimal control signals, which are duty cycles of three DC-DC converters and pitch angle of a wind turbine.

$$
\begin{aligned}
u^*(.) = \arg\underset{u(.)\in\mathbb{R}^m}{\text{minimize}} \quad & J(x(t), z(t), u(t), T) := \\
& \int_t^{t+T} \mathcal{L}(x(\tau), z(\tau), u(\tau))d\tau + \mathcal{M}(x(T), z(T)) \\
\text{s.t.: } & \mathcal{F}(x(t), \dot{x}(\tau), z(\tau), u(\tau), v(\tau)) = 0 \\
& \mathcal{H}(x(\tau), z(\tau), u(\tau)) \leq 0 \\
& \mathcal{R}(x(T), z(T)) = 0 \\
& x(\tau) = x_0, z(\tau) = z_0 \\
& \forall \tau \in [t, t+T] \\
& x(\tau) \in \mathcal{X}, z(\tau) \in \mathcal{Z}, u(\tau) \in \mathcal{U}.
\end{aligned}
\tag{10}
$$

Optimal Control Problems (OCPS): OCPs, make explicit use of the system model, given by the below functions in order to find an optimal control law u*(.), which meets number of equality and inequality constraints. The term optimal here is defined with respect to a certain criterion that implies the control objectives. This criterion is specified with a cost functional, consisting of the Lagrangian term and the terminal cost term. While the Lagrangian term indicates the cost function during the period of time, the terminal cost penalizes final values. OCPs are open-loop strategies and are wrapped by a feedback loop to construct NMPC strategies. NMPC strategies, which are also called as the receding horizon control, continuously solve an OCP over a finite-horizon using the measurements obtained at t as the initial values. Then the first optimal value is applied as the next control signal. Comparing with the conventional methods, NMPCs are inherently non-linear and multivariable strategies that handle constraints and delays. There are three different techniques to discretize and solve OCPs of the above equations [16]: 1) dynamic programming method based on the Bellman's optimality principle; 2) indirect method based on the Pontryagin minimum principle; and 3) direct methods that convert OCPs into nonlinear optimization problems (NLPs) which are then solved by NLP solvers. In this paper, a direct method, named collocation discretization, is developed in CasADi environment. CasADi implements the automatic differentiation (AD) technique [17] to reduce the controller execution time. It employs the well-known interior point optimizer (IPOPT) tool to solve the resulting NLPs.

The proposed EMS successively gets the estimated system states, ẋ, as inputs and calculates the optimal solution, U*(.), as outputs. The external state estimator and the predictor of the non-

manipulated variables are out of the scope of this paper. N step ahead predictions of the solar irradiance, wind speeds, and load demands are extracted either from a meteorological centre or an external predictor using autoregressive-moving-average (ARMA) technique. The bus voltage level of the microgrid, Vdc, is set externally and hence the developed controller can act as the secondary and primary levels of the hierarchical architecture. The developed NMPC controller consists of three entities: 1) the dynamic optimizer that successively solves OCP at each sampling time h,; 2) the mathematical model, Φ, of the system to predict its behaviour; and 3) the cost function and constraints of the relevant OCP. The optimal pitch angle, is applied as a set point to an inner closed-loop controller. Moreover, the optimal values of the switching duty cycles are applied to the pulse width modulators (PWMs) of the dc-dc converters.

4. SIMULATION AND RESULTS

To evaluate the performance of the developed optimal EMS, Two test scenarios are carried out. They are 1.) Scenario I: Constant current charging mode. 2.) Scenario II: Constant voltage charging mode.

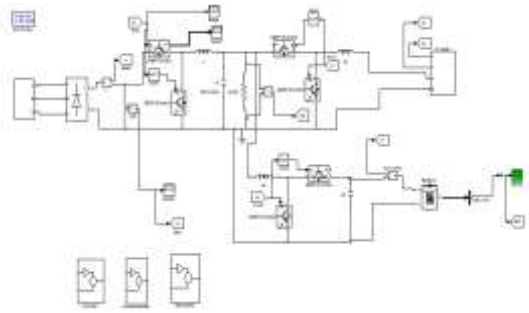

Fig 3 Proposed Simulink diagram

Scenario I: Constant Current Charging Mode:

This scenario covers the following three different cases which are run successively:

Case I: Wind turbine and PV array generate enough power at their MPPs to sup-ply load demands and charge battery bank with its nominal charging current.

Case II: The generated power is just enough to supply the load demands and therefore battery bank is not charged or is charged with the current less than its nominal charging current.

Case III: The generated power is more than the required power to supply the load demands and charge battery bank with its nominal charging current. Each case lasts for 0.05 minutes and therefore the total period of the simulation time is 0.09 minutes. In order to calculate the optimal control variables every 0.5 seconds, the developed NMPC controller runs exactly 60 times as per each case.

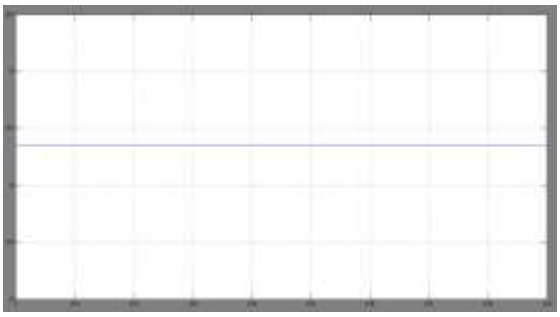

Fig. 4 PV panel voltage with MPPT control

ISSN- 2394-5125 VOL 06, ISSUE 07, 2019

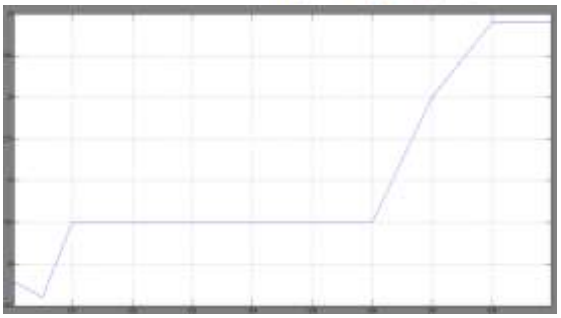

Fig. 5 PV panel voltage with NMPC control

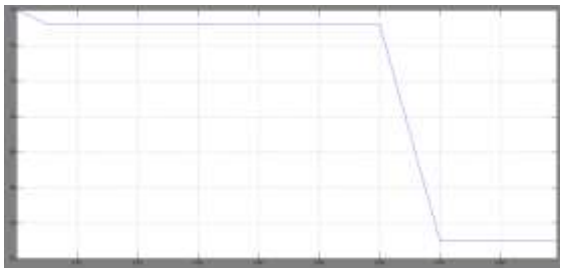

Fig 6 PV panel current with NMPC control

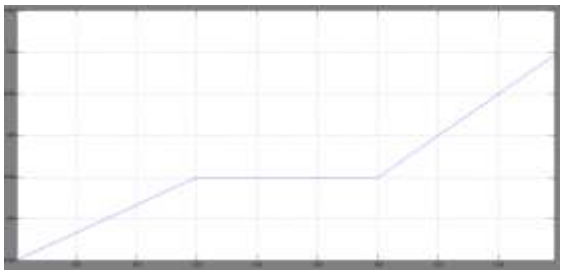

Fig 7 Battery SOC with NMPC control

Fig 8 Dc bus voltage

Scenario II: Constant voltage charging mode: Terminal voltage of battery bank rises by Scenario II due to constant charging currents. Once the battery terminal voltage level reaches its gassing voltage, charging current should be gradually reduced in order to prevent exceeding gassing voltage threshold. This constant voltage charging strategy helps battery bank to be fully charged without the risk of permanent damage. From Fig.9 , it can be seen that the developed controller switches to the constant voltage charging mode when terminal voltage of battery bank reaches to its gassing voltage.

ISSN- 2394-5125 VOL 06, ISSUE 07, 2019

Fig 9 battery voltage

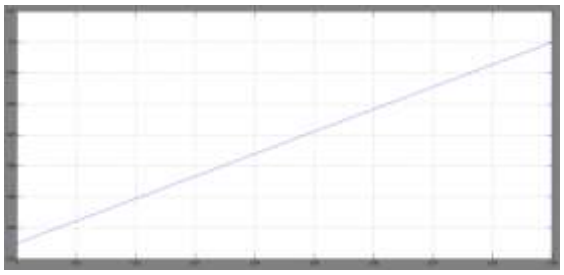

Fig.10 Battery bank SOC

5. CONCLUSION

A coordinated and multivariable online NMPC strategy has been developed to address the optimal EMS, which deals with three main control objectives of standalone dc microgrids. These objectives are the voltage level regulation, proportional power sharing, and battery management. In order to address these objectives, the developed EMS simultaneously controls the pitch angle of the wind turbine and the switching duty cycles of three dcdc converters. It has been shown that the developed controller tracks the MPPs of the wind and solar branches within the normal conditions and curtails their generations during the under load conditions. The provided flexible generation curtailment strategy realizes the constant current, constant voltage charging regime that potentially increases the life span of the battery bank. The simulation results have been shown its ability to achieve all control objectives.

REFERENCES

[1] Arash M. Dizqah, Alireza Maheri, Krishna Busawon, and Azadeh Kamjoo "A Multivariable Optimal Energy Management Strategy for Standalone DC Microgrids," IEEE transactions on power systems, vol. 30, no. 5, pp 2278-2287, September 2015.

[2] R. S. Balog, W. W. Weaver, and P. T. Krein, "The load as an energy asset in a distributed DC smart grid architecture," IEEE Trans. Smart Grid, vol. 3, no. 1, pp. 253–260, 2012

[3] J. M. Guerrero, M. Chandorkar, T. Lee, and P. C. Loh, "Advanced Control Architectures for Intelligent Microgrids-Part I: Decentralized and Hierarchical Control," IEEE Trans. Ind. Electron., vol. 60, no. 4, pp. 1254–1262, 2013.

[4] S. Anand, B. G. Fernandes, and M. Guerrero, "Distributed control to ensure proportional load sharing and improve voltage regulation in low-voltage DC microgrids," IEEE Trans. Power Electro., vol. 28, no. 4, pp. 1900–1913, 2013

[5] Chen and L. Xu, "Autonomous DC voltage control of a DC microgrid with multiple slack terminals," IEEE Trans. Power Syst., vol. 27, no. 4, pp. 1897–1905, Nov. 2012.

[6] Zhao, X. Zhang, J. Chen, C. Wang, and L. Guo, "Operation optimization of standalone microgrids considering lifetime characteristics of battery energy storage system," IEEE Trans. Sustain. Energy, Volume: 4, n0.4, pp: 934 - 943 Oct. 2013.

[7] J. M. Guerrero, J. C. Vasquez, J. Matas, L. G. de Vicua, and M. Castilla, "Hierarchical control of droop-controlled AC and DC microgrids-a general approach toward standardization," IEEE Trans. Ind. Electron., vol. 58, no. 1, pp. 158–172, 2011

[8] P. H. Divshali, A. Alimardani, S. H. Hosseinian, and M. Abedi, "De-centralized cooperative control strategy of microsources for stabilizing autonomous VSC-Based microgrids," IEEE Trans. Power Syst., vol. 27, no. 4, pp. 1949–1959, Nov. 2012.

[9] H. Fakham, D. Lu, and B. Francois, "Power control design of a battery charger in a hybrid active PV generator for load-following applications," IEEE Trans. Ind. Electron., vol. 58, no. 1, pp. 85–94, 2011

[10] X. Liu, P. Wang, and P. C. Loh, "A hybrid AC/DC microgrid and its co-ordination control," IEEE Trans. Smart Grid, vol. 2, no. 2, pp. 278–286, 2011.

[11] Meharrar, M. Tioursi, M. Hatti, and A. B. Stambouli, "A variable speed wind generator maximum power tracking based on adaptative neuro-fuzzy inference system," Expert Syst. Applicat., vol. 38, no. 6, pp. 7659–7664, 2011.

[12] O. Tremblay and L. Dessaint, "Experimental validation of a battery dynamic model for EV applications," World Elect. Vehicle Jornal., vol. 3, pp. 10–15, 2009

[13] M. Dizqah, K. Busawon, and P. Fritzson, "Acausal modeling and simulation of the standalone solar power systems as hybrid DAEs," in Proc. 53rd Int. Conf. Scandinavian Simul. Soc., 2012

[14] N. Mohan, T. M. Undeland, and W. P. Robbins, Power Electronics: Converters, Applications, and Design. New York, NY, USA: Wiley, 1995.

[15] J. H. Su, J. J. Chen, and D. S. Wu, "Learning Feedback Controller Design of Switching Converters Via MATLABSIMULINK," IEEE Transactions on Educa-tion, vol. 45, pp. 307–315, 2002.

[16] L. Grüne and J. Pannek, "Nonlinear model predictive control: Theory and algorithms," in Communications and Control Engineering. New York, NY, USA: Springer, 2011.

[17] R. Neidinger, "Introduction to automatic differentiation and MATLAB object-oriented programming," SIAM Rev., vol. 52, no. 3, pp. 545–563, 2010.